Research Journal of Engineering Sciences ISSN 2278 – 9472
Vol. **11(1),** 1-14, January **(2022)** *Res. J. Engineering Sci.*

Finite element method for relativistic analysis of wave functions of xenon atom

Rama GOMIS[1]*, Louis GOMIS[1] and Yande DIOUF[2]
[1]Plasma Physics Laboratory and Interdisciplinary Research, Dakar, Senegal
[2]Group of Solid Physics and Materials Sciences, Dakar, Senegal
rama.gomis89@gmail.com

Available online at: www.isca.in, www.isca.me
Received 28th August 2021, revised 24th November 2021, accepted 10th January 2022

Abstract

Taking into account relativistic aspect in quantum calculations, is a fundamental step towards correct modeling of systems involving heavy elements. This modeling involves an appropriate resolution of Schrödinger equation. The present study focuses on Xenon which is a heavy poly electronic atom. This is to calculate on basis of DFT, its radial wave functions for different orbitals, total energies and its effective potential in the ground state. Our motivation through this simulation is to examine the influence of relativistic effects and spin-orbit coupling on these physical grandeur. So, due to the structural complexity of the equation, we carried out the calculations implicitly by the finite element method via a program established from MATLAB software in deterministic mode. The numerical solutions obtained are based on the approximation of the local density (LDA) and that of the generalized gradient (GGA). The results obtained, allowed to describe xenon on a microscopic scale, to understand its structure and to explore the mechanisms that ensure its stability. Finally, our results are in good agreement with theoretical data found in the literature.

Keywords: Xenon, relativistic Hamiltonian, spin-orbit coupling, numerical algorithm, Schrodinger equation, MATLAB code.

Introduction

Describing behavior of electrons, atoms or molecules, was one of the main challenges for physicists at the start of the twentieth century[1]. According to the latter, it is a question of being able to calculate and predict the physical and chemical properties of these particles. Rama[2] revealed that the laws of classical mechanics are incompetent to achieve such goals. It is then up to these physicists according to Kohn[3], to appeal to the fundamental laws of quantum mechanics which govern these particles in order to characterize these properties faithfully. Adel[4] adds that the physical properties of a material, illustrated by the image of light electrons moving around heavy nuclei, depend on the behavior of its electronic structure; quantum mechanics provides the ideal framework for this. According to Nadir, Szabo and Ostlund[5,6] a good knowledge of electronic structures is an important factor for understanding the physical properties of materials. Bahnes[7] states that a good knowledge of these properties is essential for the manufacture of electronic devices and the discovery of new materials with very interesting properties. This is why, since the 1970s, the urgent search for materials with optimal optoelectronic properties have attracted the attention of the scientific community because of their many possible applications[8]. Diouf[9] studied the electronic properties of helium, carbon and iron atoms; Lamrani[10] investigated the magnetic and electronic structural properties of dilute magnetic oxides; Maylis[11] inspected the electronic and magnetic properties of iron complexes. In quantum physics, most of the work in the literature is based on the calculation of the electronic structure[12]. What makes say Susi et al.[13] that the calculations of electronic structures have become a cornerstone of modern research in chemistry and in the physics of materials, allowing the in silico modeling of chemical reactions and the design of the first principles of new catalysts. These calculations sometimes amount to solving a problem with a large number of electrons and nuclei which are in interactions. Which makes the direct resolution of Schrödinger's equation tedious or even impossible[14]. However, this resolution occupies a great center of interest in scientific research today[15,16]. The first "quantum" methods developed in this direction are, among others, those of Hartree and Hartree-Fock, which lead to the energy of the system being expressed as a functional of its wave function[4]. Using certain approximations, it amounts to transforming the famous Schrödinger equation into a system of numerically solvable equations[17]. However, these methods suffer from two drawbacks: i. they require enormous computation for a multi-electronic system and ii. they omit electronic correlation, which is the main characteristic of the quantum behavior of electrons[18]. To do this, it is necessary to use a methodology allowing the calculation of the electronic structure in principle, in a realistic way[19]. Many methods of calculating electronic structures were used before the advent of DFT. They are divided into two main categories: i. semi-empirical methods using experimental parameters and ii. ab initio methods, based on solving mathematical equations without adjusting parameters[20]. Thus, the advent of the "DFT" density functional theory has made it

possible to solve or circumvent problems. This theory, it should be remembered, is based on the two theorems of Hohenberg and Kohn-Sham, where Schrödinger equation is replaced by another equivalent[21]. The main goal of density functional theory is to replace the multielectronic wave function with electron density as the base quantity for calculations[22]. The principle consists of a reformulation of the N-body quantum problem into a unibody problem (or, strictly speaking, hatchback if we consider spin problems) with the electron density as only parameter[23]. The central idea is that the sole electron density of the ground state of the system entirely determines the mean values of observables, such as energy[24]. Originally, DFT was mainly developed within the framework of non-relativistic quantum theory (time-independent Schrödinger equation) and the Born-Oppenheimer approximation[25]. Subsequently this theory was extended to the field of time-dependent quantum mechanics (one speaks then of TDDFT for Time-Dependent Density Functional Theory) and to the relativistic field[26,27]. According to Mouhamed[28] the relativistic effects must be taken into account for a correct modeling of systems involving heavy elements. While spin-independent effects can easily be included in most quantum physics calculation codes, including spin-orbit (SO) coupling in the simulations is not trivial. One of the fundamental objectives is to describe matter on a microscopic scale in order to understand its structure and explore the mechanisms that ensure its stability[28].

However, the situation becomes more complicated when we are interested in the properties of chemical species having one or more heavy atoms, because the relativistic effects on the electronic structure become not insignificant[29,30]. These effects can be divided into two categories: the relativistic effects independent of the electron's spin, and those dependent on the spin, essentially the spin-orbit (SO) coupling[31]. Thus the treatment of all of these relativistic effects in quantum physics calculations induces the use of a relativistic Hamiltonian which, by nature, explicitly reveals the electronic spin (in opposition to the non-relativistic Hamiltonian called "spin -free")[31].

It is in this same vein that this study was initiated. It is a question of calculating on the basis of the DFT, the electronic structure of Xenon which is a heavy atom and therefore, the relativistic variation of the mass of the electrons according to the speed is not negligible any more. It then becomes relevant to take into account the corrective terms of relativistic origin in our calculations. Today, the increase in computing power and the development of increasingly efficient algorithms have contributed to the evolution of techniques for modeling materials at the atomic scale within periods that remain reasonable[14]. In the present study, the MATLAB code was used in deterministic mode to make our calculations. The results obtained, provided a better understanding of the organization of matter at the atomic scale for the case of xenon. The results are finally deemed satisfactory by comparison with experience and the literature.

Methodology

Problem definition: At the beginning of the twentieth century, physicists discovered that the laws of classical mechanics are incapable of describing the behavior of electrons, atoms or molecules[2]. Quantum mechanics provides the ideal framework for calculating and predicting the physical and chemical properties of systems with several particles (atoms or molecules)[32]. The first "quantum" methods developed in this context, are among others, those of Hartree and Hartree-Fock based on the model of independent particles[11]. These methods and those derived from this formalism are based on a multi-electronic wave function. The most common quantum physics methods are based on three approximations: i. the Born-Oppenheimer approximation which assumes that electrons adapt instantly to the motions of nuclei; ii. the approximation concerning the size of the nucleus: that is modeled by a point, this approximation has no influence as long as we are interested in valence electrons; iii. the approximation relating to the speed of the electrons: this is supposed to be sufficiently low to allow a non-relativistic description of the electrons. This hypothesis is only valid for electrons which have low kinetic energy[30]. Using these approximations, the famous Schrödinger equation is transformed into a system of numerically solvable equations. However, the methods of Hartree, Hartree-Fock and those derived, suffer from two drawbacks: one relating to the amount of computation for a multi-electronic system and the other to the omission of the electronic correlation which is the main characteristic of the quantum behavior of electrons[33]. The advent of the DFT density functional theory circumvented these problems. This theory is based on the two theorems of Hohenberg and Kohn where the Schrödinger equation is replaced by another equivalent[19]. The idea is to replace the multi-electronic wave function with electron density as the base quantity for the calculations. In other words, it consists of a reformulation of the N-body quantum problem into a unibody problem (or, strictly speaking, hatchback if we consider spin problems) with the electron density as the only parameter[14]. Thus, according to these two theorems, we can fully know the state of an electronic system by determining its electron density and we can also obtain the electron density of the ground state by minimizing the energy of the system[6]. The fundamental objective is to describe matter on a microscopic scale in order to understand its structure and explore the mechanisms that ensure its stability. However, the situation is complicated when we are interested in the properties of species with one or more heavy atoms[28]. For such atoms, the relativistic variation of the mass of an electron as a function of its speed is no longer negligible. This is because relativistic effects on physical properties such as energy are proportional to the nuclear charge of the atom concerned[34]. These effects can be divided into two categories: the relativistic effects independent of the electron's spin (scalars), and those dependent on the spin, essentially the spin-orbit (SO) coupling[35]. The origin of scalar effects is linked to the fact that electrons close to a heavy nucleus can reach speeds close to that of light, producing an effect of increasing mass[28].

The effects of spin-orbit coupling when they result from the interaction of the intrinsic magnetic moment of the electron, due to the spin, with the magnetic induction created by the orbital motion. The effect of SO coupling is manifested in several phenomena in chemistry and is notably responsible for the emergence of the ne atom structure, and it is all the more important when the nuclei are heavy. These effects of SO coupling can also influence the structure and stability of molecules[27]. The treatment of all relativistic effects (scalars and SO) in chemistry or quantum physics calculations induces the use of a relativistic Hamiltonian which, by nature, explicitly reveals the electron spin (in opposition to the non-Hamiltonian - relativist known as "spin-free")[36]. However, it can be noted that the only processing of scalar effects can be performed using scalar pseudopoentials, which is commonly implemented in most quantum computation programs. The inclusion of SO coupling requires relativistic treatment, which results in the use of a Hamiltonian involving matrices. The resulting wave function therefore involves spinors with four or two components (relativistic equivalent of the molecular orbital) with complex values. In addition, the dependence of the relativistic Hamiltonian on the spin of the electron is not without consequence because the degrees of freedom of the spin and of space are couples (via the spin-orbit operator). The result is a "mixture" of the components and the electronic spin. Ultimately, it is accepted that for a correct modeling of systems involving heavy elements, it is necessary to take into account the relativistic effects[31].

Xenon structure: Xenon is the chemical element with atomic number 54, symbol Xe. It is a noble, odorless and colorless gas. In a discharge lamp, it emits a blue light[37]. It has the particularity of being the rarest (and therefore the most expensive) gas behind argon, the latter having only radioactive isotopes[38]. Xenon is an atom whose nucleus has 54 protons and 54 electrons which constitute its electron cloud. In nature, we can find 7 stable (or almost stable) isotopes of xenon[39]. Its valence layer being completely full, it is inert with respect to most chemical reactions. Historically, xenon was discovered in 1898 by William Ramsay and Morris William Travers by spectral analysis of "residues" in air from which oxygen and nitrogen had been removed. It was Ramsay who proposed to baptize this new gas xenon, derived from the Greek word (xenos), translating as "foreigner" or "guest" because the xenon was discovered in the form of "unknown gas"[40]. The melting point corresponds to a moment of pressure and temperature at which the chemical element melts, thus passing from the solid state to the liquid state. The boiling point corresponds to a moment of pressure and temperature at which the chemical element boils, thus passing from the liquid state to the gas state[41]. In the gaseous state, its density 5.761kg.m^{-3}; in the liquid state it is 3.100g.cm^{-3} and in the solid state it is 3.640 (g.cm^{-3})[42]. The order of filling of the electronic sub shells of electrically neutral atoms in the ground state arranged by increasing atomic number is, according to the Klechkowski model:

1s → 2s → 2p → 3s → 3p → 4s → 3d → 4p → 5s →4d → 5p → 6s → 4f → 5d → 6p → 7s → 5f → 6d → 7p

The s, p, d, f sub layers can respectively contain a maximum of: 2, 6, 10 and 14 electrons. According to the Bohr model, the electrons are distributed in this order on layers called: K, L, M, N, O… which can only contain a limited number of electrons. Thus the K shell can contain a maximum of 2 electrons, the L shell, 8 electrons, the M shell, 18 electrons, the N shell, and 32 electrons…[43]. The electronic configuration of the xenon atom (54Xe) according to the Klechkowski and Bohr rules is shown in Table-1 and shown schematically in Figure-1.

Mathematical formulation: Extending DFT to the relativistic domain involves several difficulties regarding approximations of exchange and correlation energy[44]. The bases of relativistic DFT were developed in the 1970s by Rajagopal[45,46] , Von Barth and Hedin[47] and Macdonald and Vosko[48]. No relativistic methods, based on Schrödinger's Hamiltonian, rely on the approximation assuming that electrons have a sufficiently low velocity to be written in a no relativistic framework. This approximation has been found to be suitable for describing systems containing light atoms (Z<36), for which electrons have low kinetic energy[25]. However, the relativistic effects on the physical properties become not insignificant and potentially comparable to the electronic correlation for heavier atoms, so it is necessary to take them into account. Relativistic effects have their origin mainly in the fact that internal electrons are animated at a speed that can approach the speed of light and the electrons start to behave relativistically[28]. The treatment of all of these relativistic effects in quantum physics calculations induces the use of a relativistic Hamiltonian which, by nature, explicitly reveals the electronic spin (in opposition to the non-relativity Hamiltonian called "spin- free") translated by relation (1)[49].

$$\mathrm{H} = \mathrm{H}_0 + \mathrm{H}_{MV} + \mathrm{H}_D + \mathrm{H}_{SO} \tag{1}$$

The non relativistic Hamiltonian given by equation (2)

$$\mathrm{H}_0 = \sum_{i \neq j} -\frac{\Delta_i}{2} + U_i\left(r_i\right) + V_i\left(r_j\right) \tag{2}$$

The operators of the retained relativistic perturbation are given by equation (3)

$$\mathrm{H}_{MV} = -\frac{1}{4c^2}\sum_i {p_i}^4 \tag{3}$$

The mass-speed correction term is given by equation (4)

$$\mathrm{H}_D = -\frac{1}{4c^2}\sum_i^N \vec{\nabla}_i^2\left(V(r_i)\right) \tag{4}$$

Table-1: Distribution of electrons according to Klechkowski and Bohr models.

$1s^2$	$2s^2$	$2p^6$	$3s^2$	$3p^6$	$3d^{10}$	$4s^2$	$4p^6$	$4d^{10}$	$5s^2$	$5p^6$
$(K)^2$	$(L)^8$		$(M)^{18}$			$(N)^{18}$			$(O)^8$	

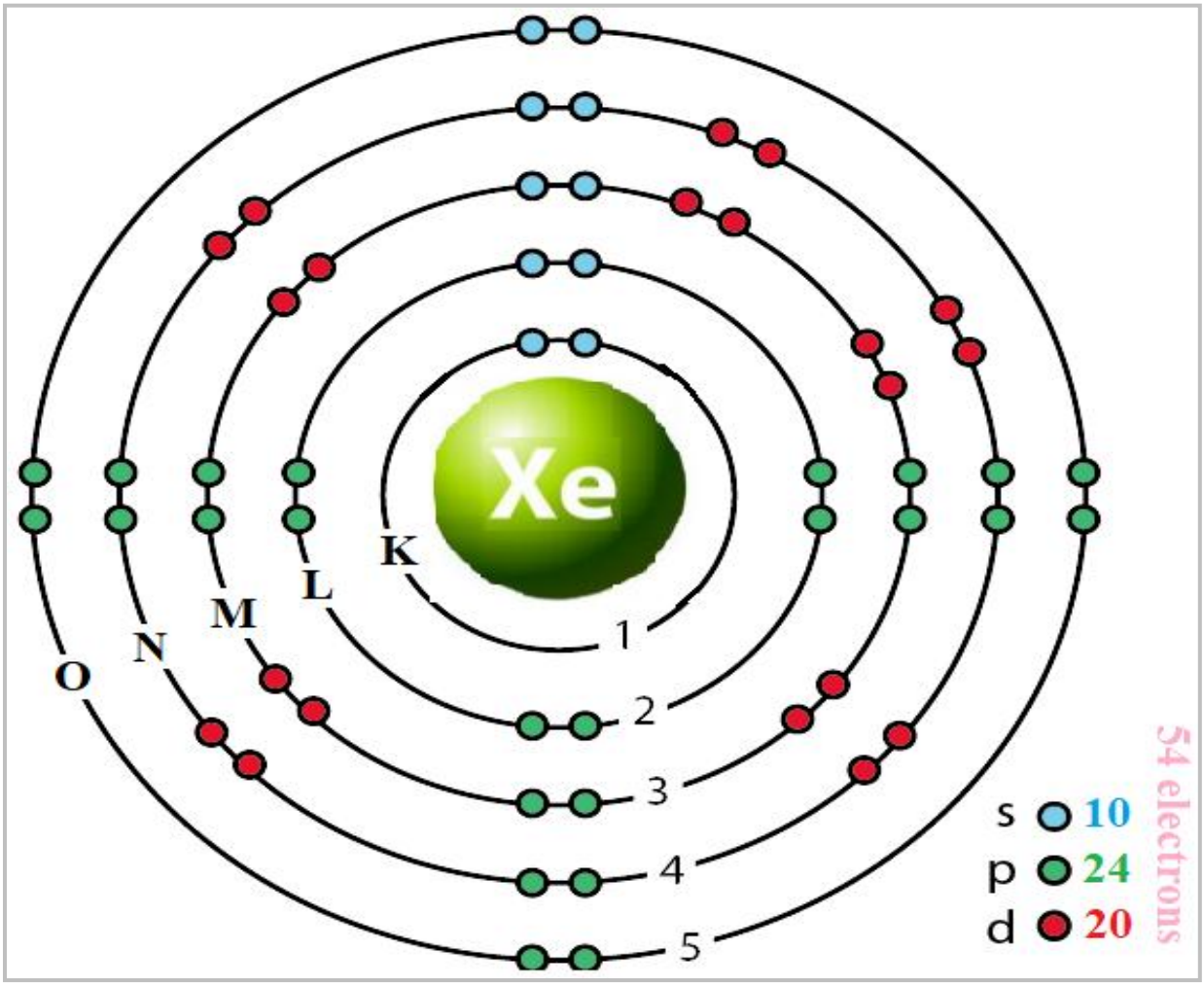

Figure-1: Disposition of electrons around the nucleus.

The term of the spin-orbit contribution is described by the expression (5)

$$\mathrm{H}_{SO} = -\frac{1}{4\,c^2}\sum_i \vec{\sigma}_i.\left(\vec{\nabla}_i V \Lambda\ \vec{p}_i\right) \tag{5}$$

Taking into account the time-independent Schrödinger equation, the relativistic Pauli equation obtained in order can be written according to the relation (6)

$$\left[\mathrm{H}_0 + \mathrm{H}_{MV} + \mathrm{H}_D + \mathrm{H}_{SO}\right]\left|\Psi\left(\vec{r}\right)\right\rangle = E\left|\Psi\left(\vec{r}\right)\right\rangle \tag{6}$$

Taking into account the previous equations, equation (8) then becomes equation (7)

$$\left[\begin{array}{l}\sum_{i\neq j} -\frac{\Delta_i}{2} + U_i\left(r_i\right) + V_i\left(r_j\right) - \frac{1}{4c^2}\sum_i p_i^4 - \frac{1}{4c^2}\sum_i^N \vec{\nabla}_i^2\left(V(r_i)\right) - \\ \frac{1}{4\,c^2}\sum_i \vec{\sigma}_i.\left(\vec{\nabla}_i V \Lambda\ \vec{p}_i\right)\end{array}\right]\left|\Psi\left(\vec{r}\right)\right\rangle = E\left|\Psi\left(\vec{r}\right)\right\rangle \tag{7}$$

Taking into account the conditions of normalization and orthogonality of wave functions, we define the total energy of a multielectronic atom with relativistic corrections and spin-orbit coupling, by relation (8)

$$E\left[\Psi\left(\vec{r}\right)\right] = \left\langle\Psi\left(\vec{r}\right)\right|\left[\sum_{i\neq j} -\frac{\Delta_i}{2} + U_i\left(r_i\right) + V_i\left(r_j\right) - \frac{1}{4c^2}\sum_i p_i^4 - \frac{1}{4c^2}\sum_i^N \vec{\nabla}_i^2\left(V(r_i)\right) - \frac{1}{4\,c^2}\sum_i \vec{\sigma}_i.\left(\vec{\nabla}_i V \Lambda\ \vec{p}_i\right)\right]\left|\Psi\left(\vec{r}\right)\right\rangle \tag{8}$$

By taking into account the properties of the operators and the orthonormalization conditions of wave functions in the development of the calculations, we end up with an expression of the energy given by equation (9)

$$E[\phi(\vec{r},\vec{\sigma})]=\sum_{\alpha}\langle\phi_\alpha(\vec{r}_i,\vec{\sigma}_i)|-\frac{\Delta_i}{2}+U_i(r_i)|\phi_\alpha(\vec{r}_i,\vec{\sigma}_i)\rangle+\frac{1}{2}\sum_{\alpha\beta}\left[\langle\phi_\alpha(\vec{r}_i,\vec{\sigma}_i)\phi_\beta(\vec{r}_j,\vec{\sigma}_j)|\frac{1}{|\vec{r}_i-\vec{r}_j|}|\phi_\alpha(\vec{r}_i,\vec{\sigma}_i)\phi_\beta(\vec{r}_j,\vec{\sigma}_j)\rangle\right.$$
$$\left.-\langle\phi_\alpha(\vec{r}_i,\vec{\sigma}_i)\phi_\beta(\vec{r}_j,\vec{\sigma}_j)|\frac{1}{|\vec{r}_i-\vec{r}_j|}|\phi_\beta(\vec{r}_i,\vec{\sigma}_i)\phi_\alpha(\vec{r}_j,\vec{\sigma}_j)\rangle\right]+\sum_{\alpha}\langle\phi_\alpha(\vec{r}_i,\vec{\sigma}_i)|-\frac{1}{4c^2}\sum_i p_i^4|\phi_\alpha(\vec{r}_i,\vec{\sigma}_i)\rangle$$
$$+\sum_{\alpha}\langle\phi_\alpha(\vec{r}_i,\vec{\sigma}_i)|-\frac{1}{4c^2}\sum_i^N\vec{\nabla}_i^2(V(r_i))-\frac{1}{4c^2}\sum_i\vec{\sigma}_i.(\vec{\nabla}_iV\wedge\vec{p}_i)|\phi_\alpha(\vec{r}_i,\vec{\sigma}_i)\rangle \quad (9)$$

By considering the stationary energy and the orthonormalization conditions satisfied, the Hartree-Fock variational principle translating the energy minimization condition can be written using Lagrange multipliers, according to equation (10)[50]

$$\delta E\left[\phi(r,\sigma)\right]-\sum_{\alpha\beta}\gamma_{\alpha\beta}\,\delta\left\langle\phi_\alpha(r,\sigma)\middle|\phi_\beta(r,\sigma)\right\rangle=0 \quad (10)$$

Où, $\phi(r,\sigma)$ est donnée par la relation (11)

$$\phi(r,\sigma)=r^{-1}P_{n\ell}(r)Y_{\ell m_\ell}\left(\theta,\varphi\right)\sigma_{m_s}\left(s_z\right) \quad (11)$$

When the normalization and orthogonality assumptions of the radial wave functions are satisfied, it is possible to write (13) in the form of equation (12)[51]

$$\delta E\left[P_{n\ell}(r)\right]-\sum_{n\ell,n'\ell}\gamma_{n\ell,n'\ell}\,\delta\left(\int P_{n\ell}(r)\,P_{n'\ell}(r)\,\mathrm{d}r\right)=0 \quad (12)$$

Thus this minimization of the total energy, combined with the respect of the conditions introducing the Lagrange multipliers, lead to the relativistic equation satisfied by the radial part of the wave function with one electron and given by the relation (13)[52]

$$\left[-\frac{1}{r^2}\left[\frac{d}{dr}\left(r^2\frac{d}{dr}\right)\right]+\frac{\ell(\ell+1)}{r^2}+V(r)-\frac{\alpha^2}{4}\left[\varepsilon_{n_0\ell_0}-V(r)\right]^2\right.$$
$$\left.-\frac{\alpha^2}{4}\left[\frac{dV(r)}{dr}\right]\frac{d}{dr}-\frac{\alpha^2}{4}\begin{pmatrix}-\ell\\ \ell+1\end{pmatrix}\left[\frac{1}{r}\frac{dV(r)}{dr}\right]\right]P_{n\ell}(r)=\varepsilon_{n\ell}\,P_{n\ell}(r) \quad (13)$$

Where $\varepsilon_{n\ell}$ represent the eigenvalues of the problem, that is, the energies of the orbitals. In practice, DFT methods use the Kohn-Sham approach[53]. This approach considers that the electrons must be immersed in an effective external potential. It thus made it possible to explicitly separate the kinetic term and the Hartree term from the exchange-correlation term. It follows that the potential $V(r)$ contained in the radial relativistic equation (15) can be approximated by the effective potential $V_{eff}(r)$ Therefore, the Kohn-Sham equation with relativistic corrections and spin orbit coupling is written according to equation (14)[54].

$$\left[-\frac{1}{r^2}\left[\frac{d}{dr}\left(r^2\frac{d}{dr}\right)\right]+\frac{\ell(\ell+1)}{r^2}+V_{eff}(r)-\frac{\alpha^2}{4}\left[\varepsilon_{n_0\ell_0}-V_{eff}(r)\right]^2\right.$$
$$\left.-\frac{\alpha^2}{4}\left[\frac{dV_{eff}(r)}{dr}\right]\frac{d}{dr}-\frac{\alpha^2}{4}\begin{pmatrix}-\ell\\ \ell+1\end{pmatrix}\left[\frac{1}{r}\frac{dV_{eff}(r)}{dr}\right]\right]P_{n\ell}(r)=\varepsilon_{n\ell}\,P_{n\ell}(r) \quad (14)$$

It is a question of finding the solutions of this equation, the analytical resolution of which is difficult, if not impossible. It is then up to the use of digital methods calling on adequate computer resources.

Numerical procedure: In order to be able to approach the numerical resolution of the equations of Kohn and Sham, we rewrite the equation (16) in the form of a differential equation translated by the relation (15)

$$\left[-\frac{1}{r^2}\left[\frac{d}{dr}\left(r^2\frac{d}{dr}\right)\right]+\frac{\ell(\ell+1)}{r^2}+W(r)-\frac{\alpha^2}{4}\left[\frac{dV_{eff}(r)}{dr}\right]\frac{d}{dr}-\frac{\alpha^2}{4}\begin{pmatrix}-\ell\\ \ell+1\end{pmatrix}\left[\frac{1}{r}\frac{dV_{eff}(r)}{dr}\right]-\varepsilon_{n\ell}\right]P_{n\ell}(r)=0 \quad (15)$$

Where we set W (r) as a potential defined by relation (16)

$$W(r)=V_{eff}(r)-\frac{\alpha^2}{4}\left[\varepsilon_{n_0\ell_0}-V_{eff}(r)\right]^2 \quad (16)$$

$\varepsilon_{n\ell}$ is a bound state called orbital energy. In order for these energies ε_{nl} to describe a correct energy spectrum, we impose boundary conditions on the potential[55].

For the resolution, we used the finite difference method to find the numerical solutions of equation (15). In reality, the calculation took place iteratively using a self-consistent cycle according to 6 steps: i. choice of input potential W^{input} ii. calculation of the effective Kohn-Sham potential $V_{eff}(r)$ iii. solving the relativistic Kohn-Sham equation, iv. calculation of the output potential $W(r)$ v. verification of the convergence criterion of the solutions (by comparing the input potential W^{input} and the output one, $W(r)$). If the criterion is not yet satisfied, we start the cycle again. The most widely used convergence criteria are based on the difference between the energies corresponding to the α^{th} and $(\alpha-1)^{th}$ iteration as shown by equation (17)

$$\left|\varepsilon_\alpha-\varepsilon_{\alpha-1}\right|\prec\eta \quad (17)$$

η, being the tolerance value (details) that we choose from the start. vi. calculation of the various physical quantities involved; End of process.

All of these steps are shown schematically by the algorithm shown in Figure-2.

Due to the structural complexity of the system, the basic equations were implicitly linearized and solved numerically by the finite element method using Matlab software. MALAB (MATrix LABoratory) is programming software that makes it as easy as possible to transcribe a mathematical problem into computer language, using writing as close as possible to scientific natural language. A sequential resolution of the problem with the help of this computer program made it possible to quickly obtain interesting results which were difficult, if not impossible, to obtain with other approaches such as the analytical one.

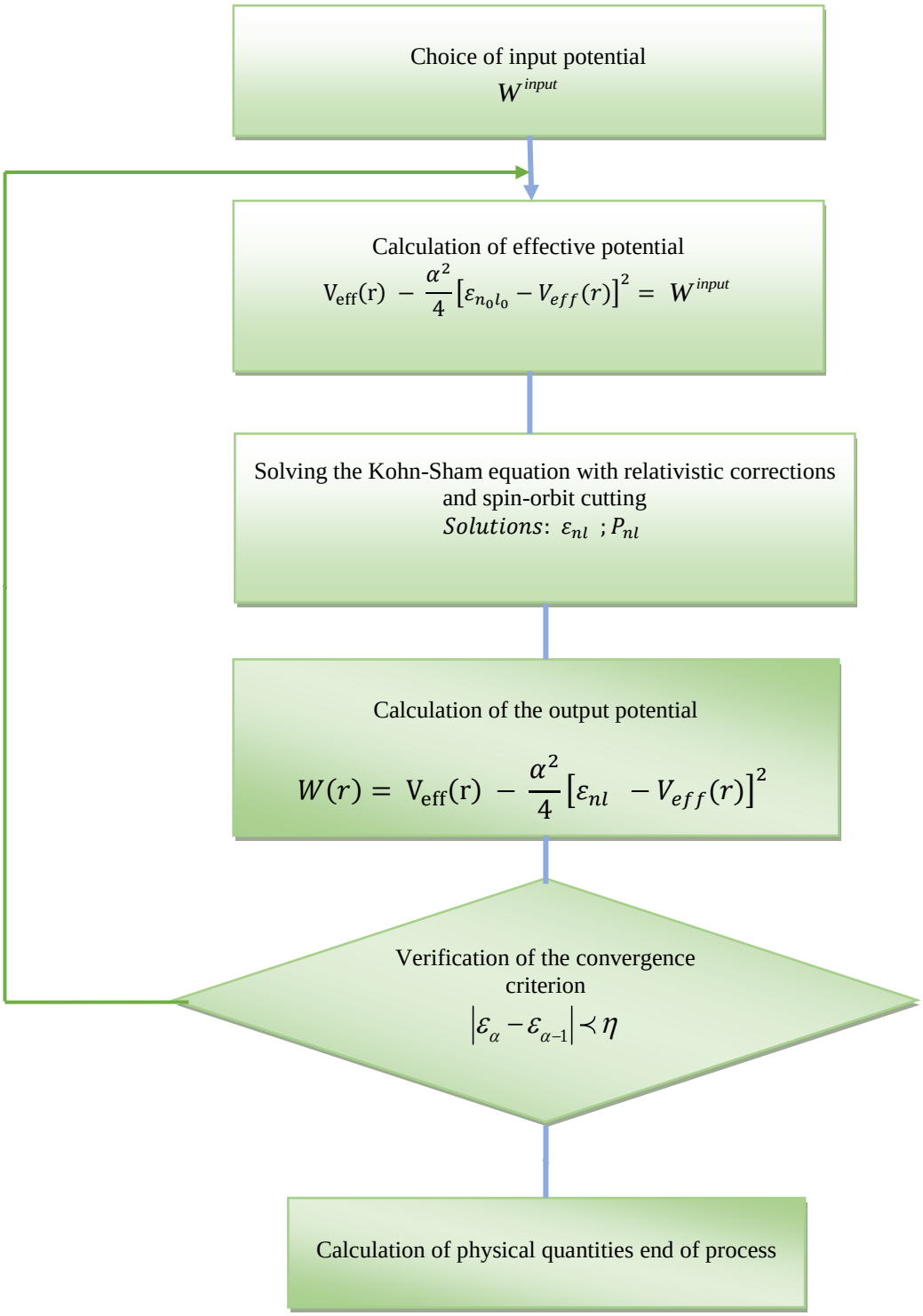

Figure-2: Iterative process used in solving the relativistic Kohn-Sham equation.

Results and discussion

The results that we will present here are obtained with calculations based on the local density approximation (LDA) and the generalized gradient approximation (GGA). Only the terms of the Vosko-Wilk-Nusser exchange-correlation potential (VWN) and the correlation exchange potential of Perdew, Burke and Ernzerhof (PBE) are considered for the LDA and GGA respectively. We will limit ourselves here to the results relating to the distribution of the radial wave function for s, p and d orbitals, to the effective potential and to the total energies of the xenon atom in the ground state.

Radial wave function: For s orbitals: In Figures-3a, 3b, 3c, 3d and 3e, we can see the variations in the radial wave function of the 1s, 2s, 3s, 4s, and 5s orbitals, respectively. The analysis of Fig. 3a shows that the radial wave function tends towards zero in the vicinity of the nucleus and out of its field of action, for rays tending to infinity. The function admits a maximum in the neighborhood of r=0.01 u.a; which corresponds to the most probable position to find an electron from shell 1s. In the immediate vicinity and far from the nucleus, the probability of finding an electron is very low or even almost zero. Far from the nucleus, the interaction potential tends to zero, while near the nucleus the force of repulsion is so great that the electron cannot cross a limit barrier. This variation of the radial wave function of the 1s orbital of the xenon ground state respects the finitude conditions of atomic wave functions. The two methods used look the same. Unlike the 1s orbital given by Figure-3a, the 2s, 3s, 4s, and 5s orbitals, (represented respectively by figures 3b, 3c, 3d and 3e), form a wave structure which gives probable positions to find, in these areas the sign of the wave function will be either positive or negative but the probability remains positive. We also notice that the greater the quantum number n, the more nodes we have; let (n-l-1) nodes. For the 2s orbital, the maximum is in the vicinity of r = 0.02 u.a; for the 3s orbital, we have two maximums: at r = 0.01 u.a and r = 0.25 u.a; for the 4s orbital, we note two maximums: at r = 0.01u.a and r = 0.3 u.a and the 5s orbital which has three maximums: at r = 0.01u.a and r=1.5 u.a. All these variations tend towards zero for large values of r. for the two methods chosen, the curves present practically the same appearance except for the variation of the 5s orbital where the curve of the so-called Perdew-Burke-Ernzerhof method deviates slightly from that of the LDA-VWN. The 5s orbital being a valence layer, the correlation exchange phenomena are more accentuated.

For p orbitals: Figures-4a, 4b, 4c and 4d illustrate the distribution of the radial wave functions of the 2p, 3p, 4p, and 5p orbitals, respectively. So apart from the 2p orbital, (Figure-4a), the other 3p, 4p, and 5p orbitals (Figures-4b, 4c and 4d), all have nodes with a total number of n_l- 1. There is a succession of maximum and minimum of the radial wave functions, which corresponds to the most probable values of the regions to locate the electrons. All the curves tend towards zero for the large r, that is to say outside the range of the nucleus. For the two methods chosen, the curves present practically the same shape except for the variation of the 5p orbital where the curve of the so-called Perdew-Burke-Ernzerhof method deviates slightly from that of the LDA-VWN. Like the 5s orbital, the 5p orbital is also a valence layer, so the exchange-correlation phenomena are also more pronounced there.

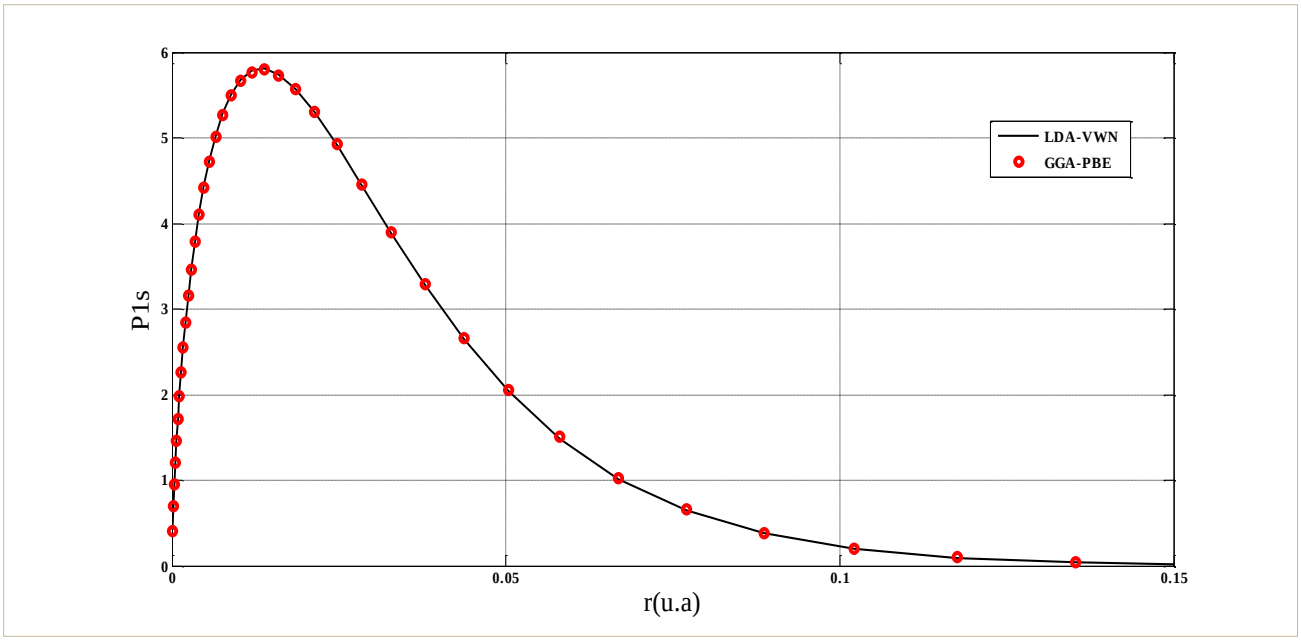

Figure-3a: Variation of radial wave function of 1s orbital of xenon atom in its ground state.

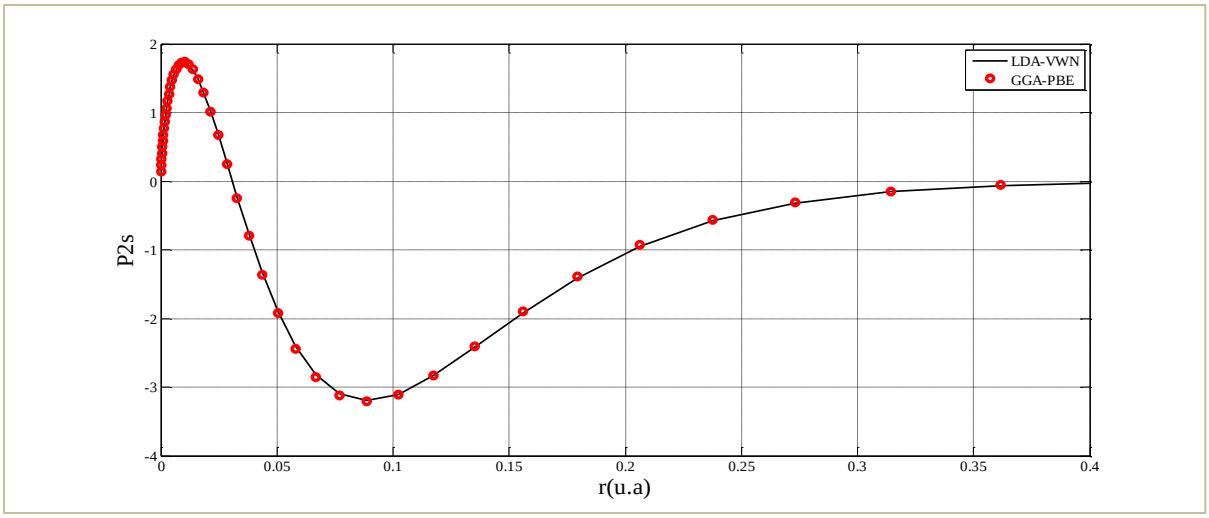

Figure-3b: Variation of radial wave function of 2s orbital of xenon atom in its ground state.

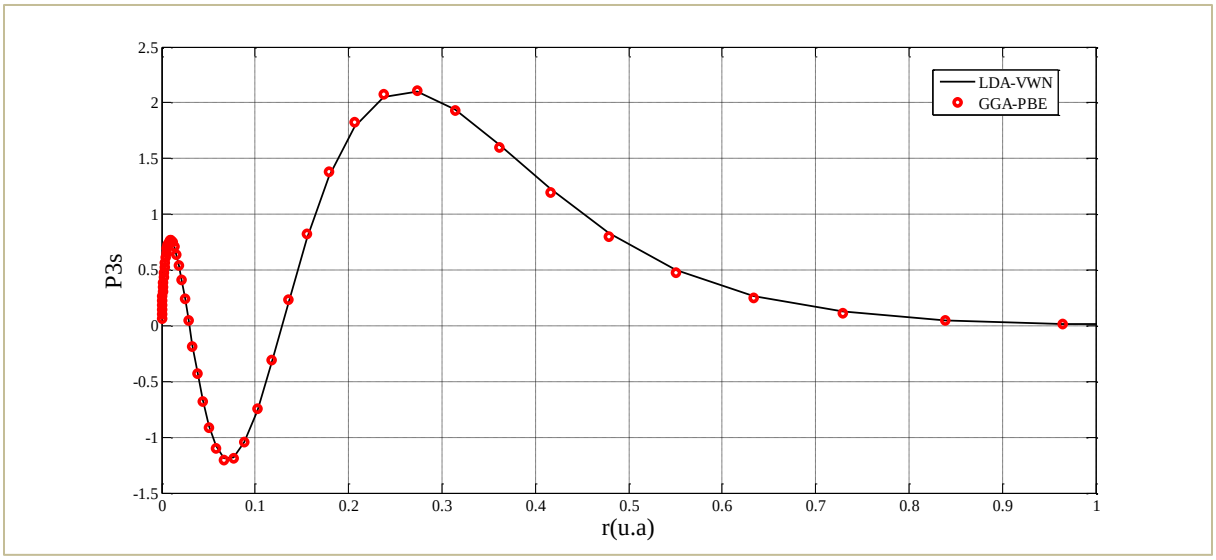

Figure-3c: Variation of radial wave function of 3s orbital of xenon atom in its ground state.

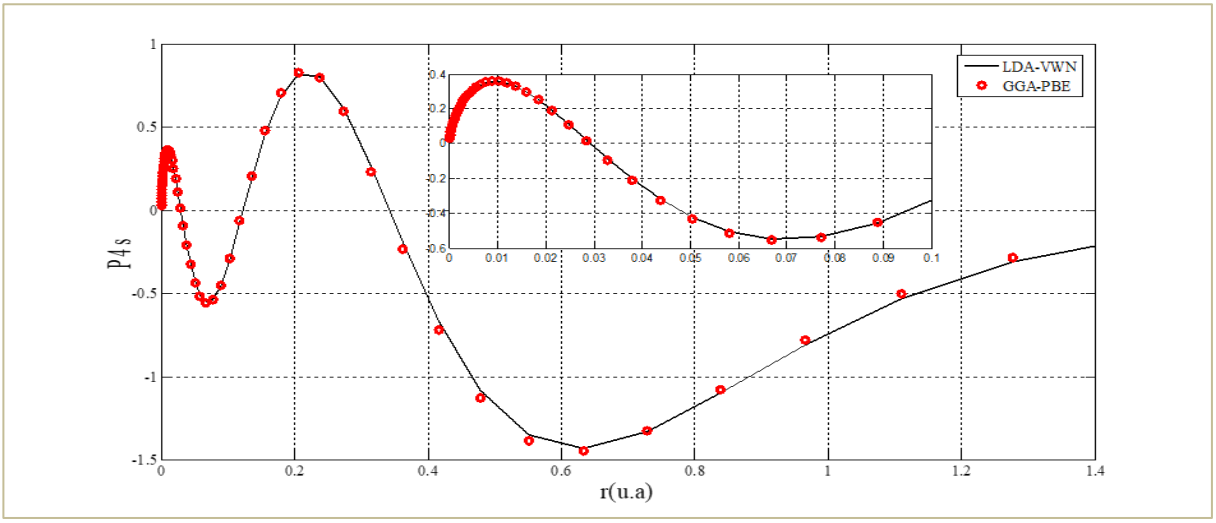

Figure-3d: Variation of radial wave function of 4s orbital of xenon atom in its ground state.

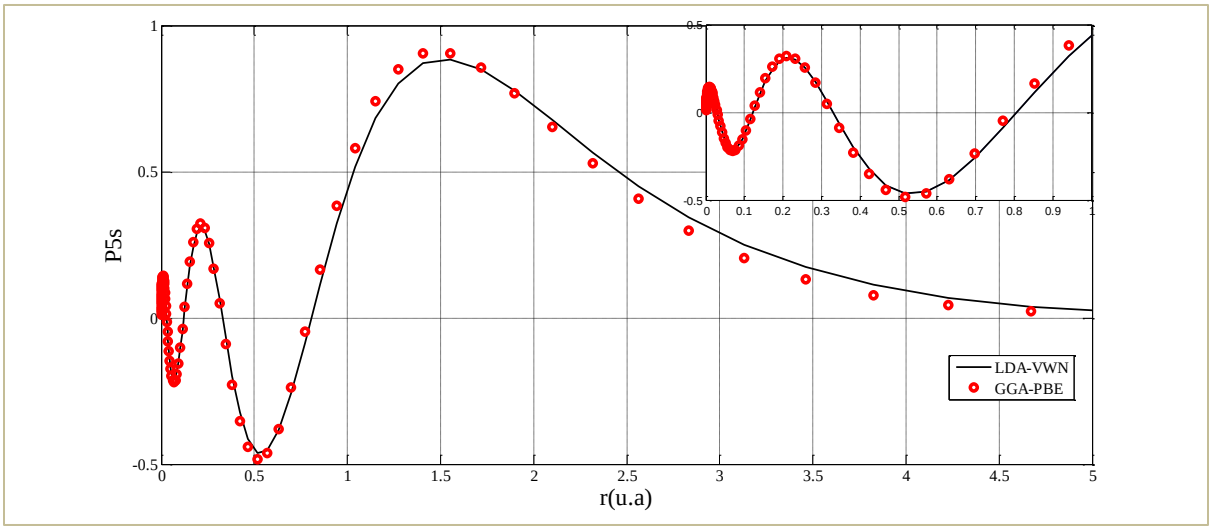

Figure-3e: Variation of radial wave function of 5s orbital of xenon atom in its ground state.

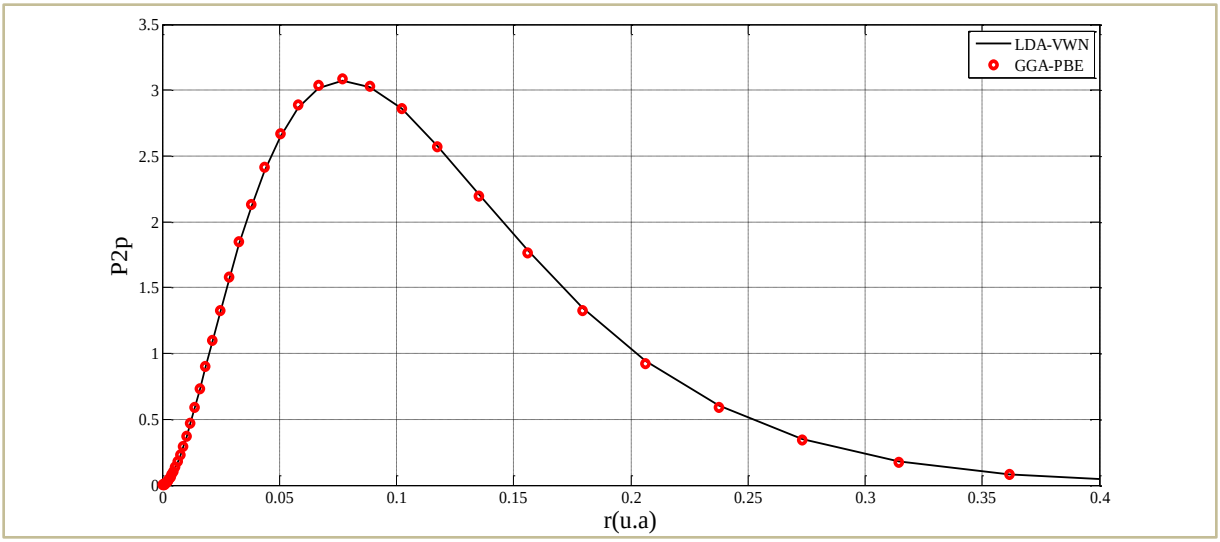

Figure-4a: Variation of radial wave function of 2p orbital of xenon atom in its ground state.

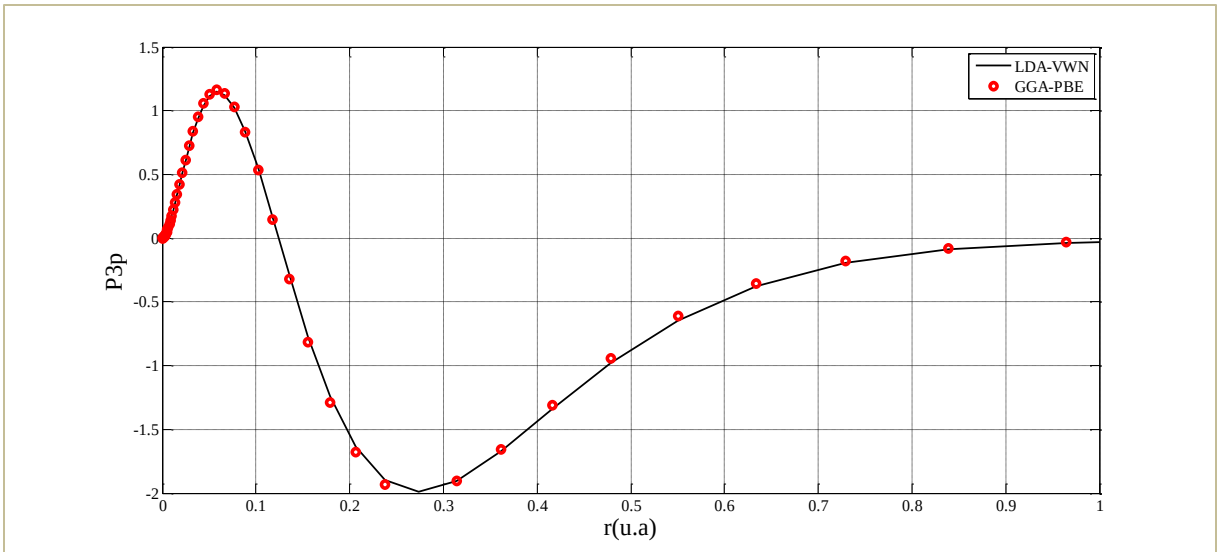

Figure-4b: Variation of radial wave function of 3p orbital of xenon atom in its ground state.

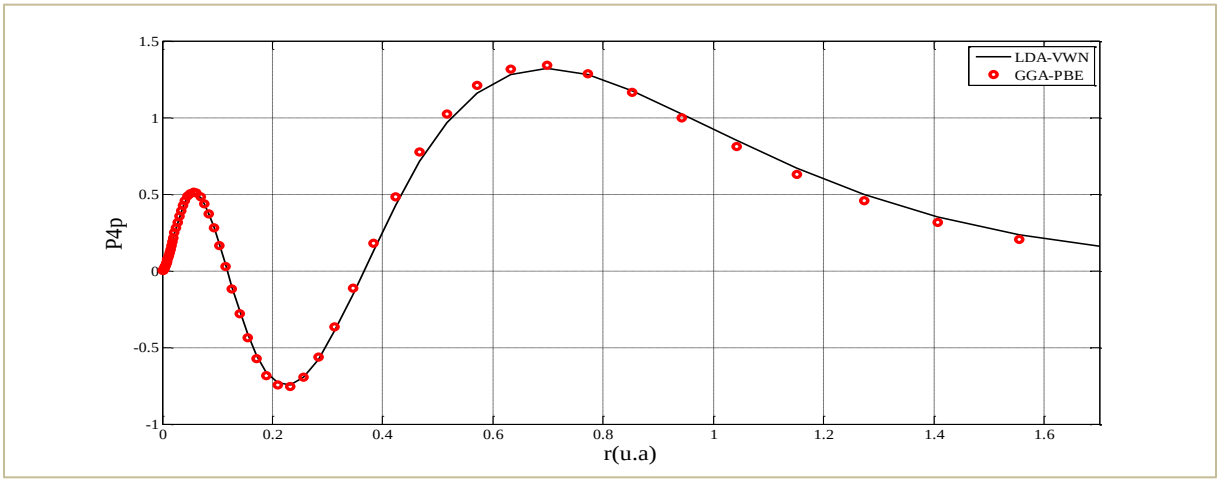

Figure-4c: Variation of radial wave function of 4p orbital of xenon atom in its ground state.

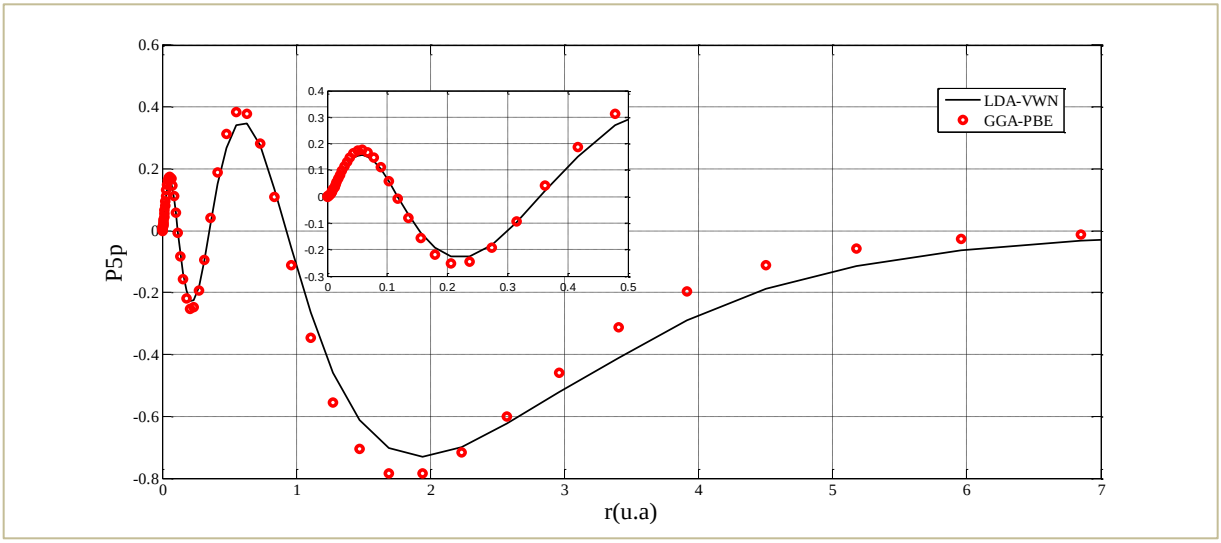

Figure-4d: Variation of radial wave function of 5p orbital of xenon atom in its ground state.

For d orbitals: Figure-5a and 5b show the evolution of the radial wave function of 3d and 4d orbitals respectively. The analysis shows that the radial wave function of the 3d orbital (Figure-5a), tends towards zero in the vicinity of the nucleus and out of its field of action for the rays tending towards the nucleus. infinite. This function admits a maximum in the neighborhood of r=0, 21u.a, which corresponds to the most probable position to find an electron from the 3d shell. For the 4d orbital (Figure-5b), the variation has a knot. The probability of presence is maximum in the neighborhood of r = 0.2u.a and r = 0.7u.a, it tends towards zero when r increases.

Effective potential: Figure-6 shows the variation of the effective potential of the xenon atom in its ground state obtained in each approach. Note that the two curves representing the variation of the potential tend towards zero when the gap between the nucleus and the electrons is large. This is explained by the weak influence of the nucleus on the electrons if the latter move away. The two potential curves obtained by the local Vosko-Wilk-Nusser method approach and that obtained by the generalized gradient approach, Perdew-Becke-Ernzerh of method present practically the same shape.

Total energies: We present in Table-2, the total energies of the xenon atom obtained numerically in the context of our study. Our results are then compared with the theoretical results of Bunge, C. F. and Barrientos, J. A.[56] for the same atom. In this table, the relative deviations are also shown. By analyzing the data in the Table above, we notice that the results obtained in the Vosko-Wilk-Nusser local density approach have a small difference (3.5% for the total energy) between the numerical data obtained in the framework of our work and the data extracted from the work of Bunge, C. F. and Barrientos, J. A.[56].

In contrast, the disagreement between the total energy in the Perdew-Burke-Ernzerhof generalized gradient method and the total energy determined by Bunge, C. F. and Barrientos, J. A.[56] is around 6.1%.

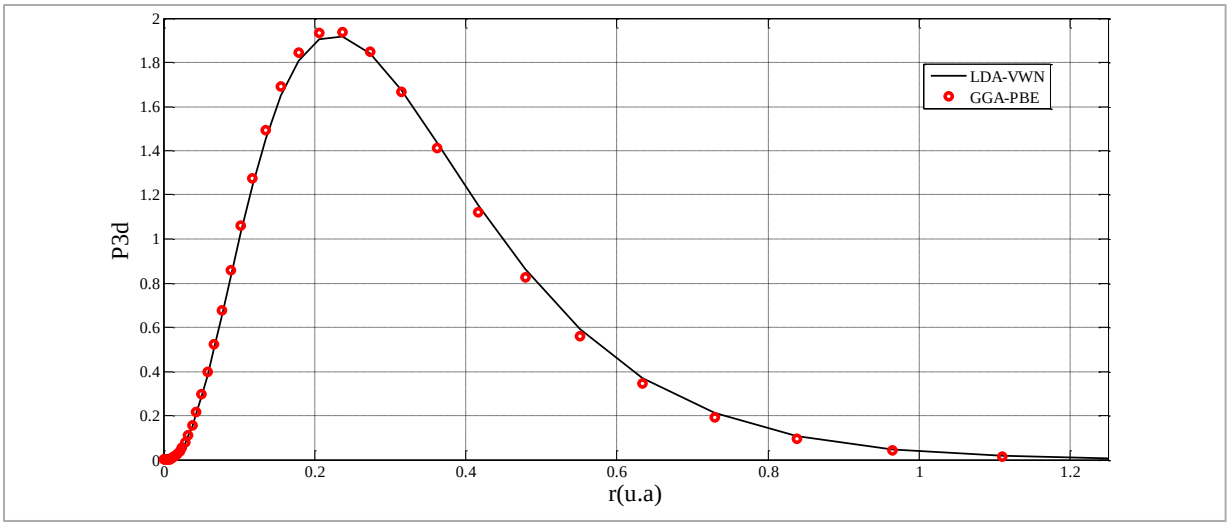

Fig.5a. Variation of the radial wave function of the 3d orbital of the xenon ground state.

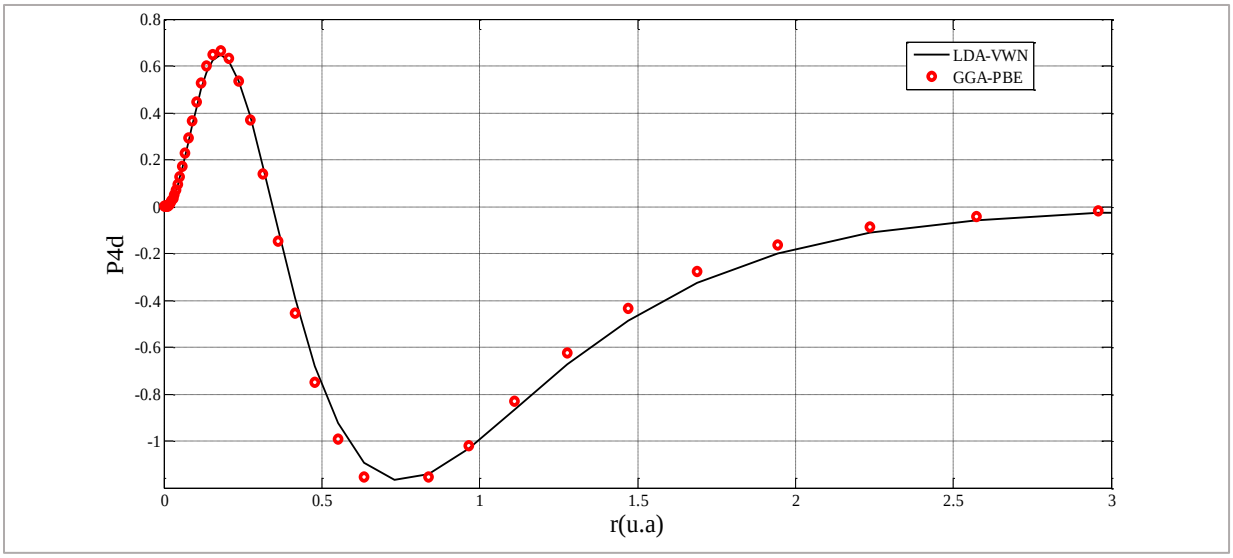

Figure-5b: Variation of radial wave function of 4d orbital of xenon atom in its ground state.

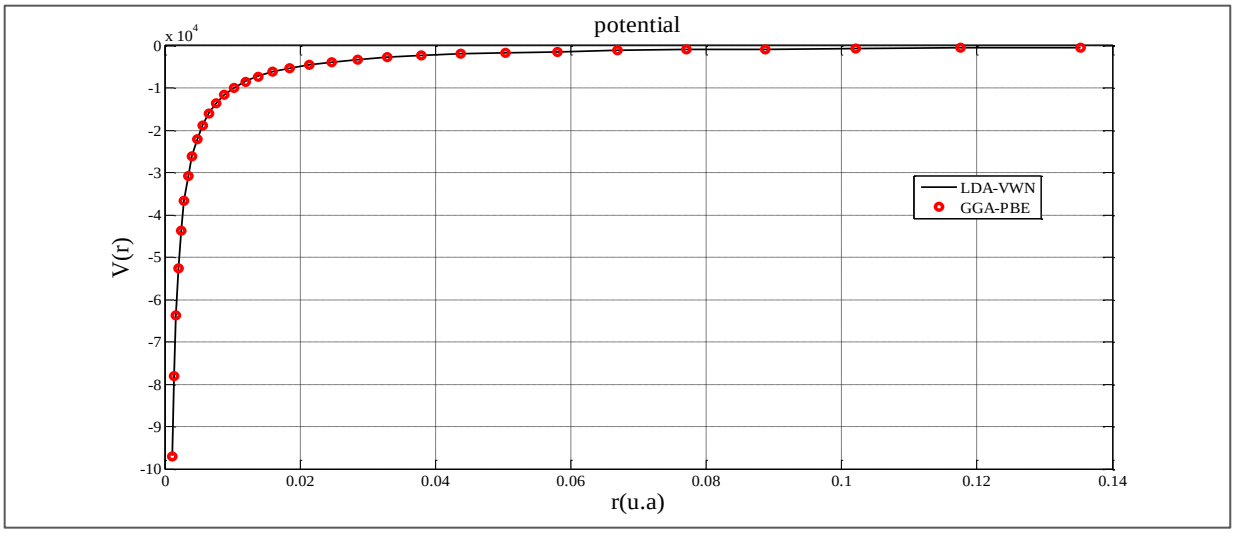

Figure-6: Variation of effective potential of xenon atom in its ground state.

Table-2. Comparison of total energies in the so-called**:** LDA-VWN, GGA-PBE et RHF.

	Results of Bunge C. F. and Barrientos, J. A.[56] (RHF)	LDA-VWN	$\delta_1(\%)\ LDA^{VWN}$ -RHF	GGA-PBE	$\delta_2(\%)\ GGA^{PBE}$ -RHF
$E_{tot}(u.a)$	-7232,13849	-7485,5	3,5032	-7677	6,1511

Conclusion

One of the great attractions of DFT methods is the resolution of the Schrödinger equation including corrective terms of relativistic origin. In this work, we were interested in xenon, a heavy atom that has 54 electrons. The structural complexity of the equation required the development of a MATLAB code used in deterministic mode to do our calculations. These calculations focused on physical quantities such as the radial wave functions, the total energies and the effective potential in the ground state based on the approximation of the local density (LDA) and that of the generalized gradient (GGA). At the end of the study, the results obtained are consistent and meaningful. For the 1s orbital, the radial wave function tends to zero in the vicinity of the nucleus and out of its field of action, for rays tending to infinity. It admits a maximum in the neighborhood of r=0.01 u.a; corresponding to the most probable position to find an electron from shell 1s. In the immediate vicinity and far from the nucleus, this probability is very low or even almost zero. Far from the nucleus, the interaction potential tends to zero, while near the nucleus the force of repulsion is so great that the electron cannot cross a limit barrier. For the 2s, 3s, 4s, and 5s orbitals, we note a wave structure giving positions likely to be found, in these areas the sign of the wave function will be either positive or negative but the probability remains positive. We also notice that the greater the quantum number n, the more nodes we have; let (n-l-1) nodes. For the 2s orbital, the maximum is in the neighborhood of r=0.02 u.a; for the 3s orbital, we have two maximums: at r=0.01 u.a and r=0.25 u.a; for the 4s orbital, which also has two maximums, we have r = 0.01u.a and r=0.3 u.a and finally for the 5s orbital, we note three maximums: at r=0.01u.a and r=1.5 u.a. All these variations tend towards zero for large values of r. For the two methods chosen, the curves present practically the same appearance except for the variation of the 5s orbital where the curve of the so-called Perdew-Burke-Ernzerhof method deviates slightly from that of the LDA-VWN. The 5s orbital being a valence layer, the correlation exchange phenomena are more accentuated. Apart from the 2p orbital, the other 3p, 4p, and 5p orbitals all have nodes totaling n-1-1. There is a succession of maximum and minimum radial wave functions, corresponding to the most probable values of the regions to locate the electrons. All the curves tend towards zero for large r, that is, outside the range of the nucleus. For the two methods chosen, the curves present practically the same appearance except for the variation of the 5p orbital where the curve of the so-called Perdew-Burke-Ernzerhof method deviates slightly from that of the LDA-VWN. Like the 5s orbital, the 5p orbital is also a valence layer, so the exchange-correlation phenomena are also more pronounced there. For the 3d orbital, the radial wave function tends to zero in the vicinity of the nucleus and out of its field of action for rays tending to infinity. This function admits a maximum in the neighborhood of r= 0.21u.a, which corresponds to the most likely position of finding an electron from the 3d shell. For the 4d orbital, the variation has a knot. The probability of presence is maximum in the neighborhood of r = 0.2u.a and r = 0.7 u.a, it tends towards zero when r increases. For the effective potential, the variation tends to zero when the gap between the nucleus and the electrons is large. This is explained by the weak influence of the nucleus on the electrons if the latter move away. The two potential curves obtained by the local Vosko-Wilk-Nusser method approach and that obtained by the generalized gradient approach, Perdew-Becke-Ernzerhof method present practically the same shape. Finally for the total energies, the relative differences between our results and those of 56 show that the results obtained in the Vosko-Wilk-Nusser local density approach have a small difference (3.5% for the total energy). By cons, the disagreement between the total energy in the Perdew-Burke-Ernzerhof generalized gradient method and the total energy determined by 56 is around 6.1%. In short, the results obtained made it possible to better understand the organization of matter at the atomic scale for the case of xenon. Finally, they are considered satisfactory by comparison with experience and the literature. This study concerns the xenon atom only in the fundamental state; thus to give this study its full relevance, it is imperative to extend the study to excited states.

Acknowledgements

I benefited from the scientific and educational expertise of Dr V.B. Traore. I would like here to magnify to him all my gratitude for his spirit of sharing.

References

1. Gonze, X., Beuken, J., M., Caracas, R., Detraux, F., Fuchs, M., Rignanese, G., M., Sindic, L., Verstraete, M., Zerah, G., Jollet, F., Torrent, M., Roy, A., Mikami, M., Ghosez, Ph., Raty, J., Y., and Allan., D., C. (2002). First-principles computation of material properties: the ABINIT software project. *Comp. Mat. Sci*., 25, 478-492.

2. Rama, G. (2019). Density Functional Theory (DFT) in the study of relativistic corrections and spin-orbit coupling. Application to the electronic structure of xenon, Master's thesis, Cheikh Anta Diop University of Dakar.

3. Kohn, W. (1999). Nobel Lecture: Electronic structure of matter - wave functions and density functional. *Rev. Mod. Phys*, 71, 1253.

4. Adel, F. A. A. (2009). Modeling within the DFT of the

properties of electronic and magnetic structures and of chemical bonding of Intermetallic Hydrides. Thesis, University of Bordeaux I.

5. Szabo, A and Ostlund, N. S. (1989). Modern quantum chemistry: introduction to advanced electronic structure theory. Courier Corporation.

6. Nadir, M. (2014). Study of the physical properties of transition metal nanostructures: CunNim. Master's thesis in Physics and Nano composites, University A. MIRA - Béjaïa.

7. Bahnes, A. (2014). Study of two first-principle methods applied to the Heuslers. Master's thesis, USTO-MB, Algeria.

8. Nabil, B.B.E. (2013). Ab-initio study of the structural and electronic properties of ternary alloys of zinc-based II-VI semiconductors, These De Physique Theorique, Uni. Abou Bakr Belkaïd - Tlemcen, Morocco.

9. Diouf, Y. (2017). Theoretical study of the electronic structure of multielectronic atoms in the approximation of the density functional theory. Master's Thesis in Physics and Applications, Cheikh Anta Diop University of Dakar**.**

10. Lamrani, F. (2015). Modeling and simulation by DFT of the electronic magnetic and structural properties of diluted magnetic oxides. Ph.D. Thesis in computational physics, University Rabat Mohammed V, Morocco.

11. Maylis, O. (2007). Density Functional Theory study of electronic and magnetic properties of iron complexes. *Application to Catalase and Iron-Sulfur type systems*. Other, Joseph-Fourier University - Grenoble.

12. Poree, C., & Schoenebeck, F. (2017). A holy grail in chemistry: Computational catalyst design: Feasible or fiction?. *Accounts of chemical research*, 50(3), 605-608.

13. Lehtola, S., Blockhuys, F., & Van Alsenoy, C. (2020). An overview of self-consistent field calculations within finite basis sets. *Molecules*, 25(5), 1218.

14. Diouf, Y., Talla, K., Diallo, S., and Gomis, L. (2021). Numerical Study of Density Functional Theory of Multi-electronic Atoms: Case of Carbon and Helium. *American J. of Nano.* 9(1), 12-22.

15. Shamim, M. D. and Harbola, M. K. (2010). Application of an excited state LDA exchange energy functional for the calculation of transition energy of atoms within time independent density functional theory. *J.of Phys. B: Atomic, Molecular and Optical Physics*, 43(21), 1-12

16. Jones, R. O. (2015). Density functional theory: Its origins, rise to prominence and future. *Rev. of Mod. Phys.*, 87(3), 897-923.

17. Xiao, D. W., Richard, L. M., Thomas, M. H. and Gustavo, E. S. (2013). Density Functional Theory Studies of the Electronic Structure of Solid State Actinide Oxides. *Chem. Rev*, 113 (2), 1063–1096.

18. Evangelista, F. A., Shushkov, P., & Tully, J. C. (2013). Orthogonality constrained density functional theory for electronic excited states. *The Journal of Physical Chemistry A*, 117(32), 7378-7392.

19. Chloé, N. G. (2019). Study of the electronic, magnetic and magnetocaloric properties of La2MnBO6 (B = Ni, Ru, Co, Fe) and LaAMnFeO6 (A = Ba, Sr, Ca) materials and their potential for magnetic refrigeration. Master's thesis, Sherbrooke, Quebec.

20. Ravo, T. R., Raoelina, A., Hery, A. and Rakotoson, H. (2018). Density Functional Theory and its applications in Nanotechnology. Communication made during the first international conference on Nanotechnology in Madagascar, pp 11-12.

21. Tang, Q., Zhen, Z. and Zhongfang, C. (2015). Innovation and discovery of graphene-like materials via density-functional theory computations. *WIREs Comput Mol Sci*, 5(5), 360–379.

22. Yousef, S., James, R. C. and Suzanne, M. S. (2010). Numerical methods for electronic structure calculations of materials. *SIAM Review*, 52(1), 3-54.

23. Kohn, W. (1996). Density Functional and Density Matrix Method Scaling Linearly with the Number of Atoms. *Phys. Rev. Letters*, 76(17), 3168–3171.

24. Blackburn, S. (2013). Analysis of the electronic properties of superconductors using the density functional theory. Thesis, University of Montreal.

25. Dyall, K. G. and Fægri, K. (2007). Introduction to Relativistic Quantum Chemistry. Oxford University Press

26. Kohn, W., Becke, A. D. and Parr, R. G. (1996). Density Functional Theory of Electronic Structure. *J. Phys. Chem.* 100 (31), 12974–1298.

27. Marian, C. M. (1997). Fine and Hyper fine Structure In Problem Solving in Computational Molecular Science. *Springer*, 29-35.

28. Mouhamed, A. (2016). Applications of ELF and QTAIM topological approaches in an almost relativistic 2-component context. Doctoral thesis, Pierre and Marie Curie University.

29. Han, Y. K. and Lee, Y. S . (1999). Structures of RgFn (Rg = Xe, Rn, and Element 118. n = 2, 4.) calculated by two-component spin-orbit methods. A spin-orbit induced isomer of (118) F4. *J Phys Chem A*, 103(8), 1104–1108.

30. Danilo, C. (2009). Theoretical modeling of solvated actinide spectroscopy. Theoretical modeling of actinide spectra in solution, Doctoral thesis, University of Lille 1 - Stockholm University.

31. Zhao, M., Xu, S., Shanshan, N. and Xiangjun, C. (2017). Relativistic and distorted wave effects on Xe 4d electron momentum distributions. *Chinese Physics B*, 26(9), 093103-4

32. Bader, R. F. (1990). Atoms in molecules: a quantum theory. Inter. series of monographs on chemistry 22.

33. Parr, R. G. and Yang, W. (1989). Density-Functional Theory

of Atoms and Molecules. Oxford University Press.

34. Wullen, C. V. (2010). Relativistic density functional theory In Relativistic methods for chemists. *Springer*, 191-214.

35. Sarrio, C. C., Vallet, V., Maynau, D. and Marsden, C. J. (2004). Can density functional methods be used for open-shell actinide molecules: Comparison with multiconfigurational spin-orbit studies. *J. Chem. Phys*, 121(11), 5312.

36. Hess, B. A. and Marian, C. M. (1999). Chapter1-Relativistic effects in the calculation of clectronic energies, computational molecular spectroscopy, John Wiley & Sons, Wiley, Sussex.

37. Neil, B. (2003). The Noble Gases. Chemical & Engineering News. *American Chem. Soci*., 81(36).

38. Martin B. K. and Christoph, P. (2006). Isotopic signature of atmospheric xenon released from light water reactors. *J. of Envi. Radioactivity*, 88(3), 215-235.

39. Mahaffy, P. R., Niemann, H. B., Alpert, A., Atreya, S. K., Demick, J., Donahue, T. M., Harpold, D. N and . Owen, T. C. (2000). Noble gas abundance and isotope ratios in the atmosphere of Jupiter from the Galileo Probe Mass Spectrometer. *J. of Geo. Research*, 105(6), 15061–15072.

40. Ramsay, W. (1902). An Attempt to Estimate the Relative Amounts of Krypton and of Xenon in Atmospheric Air. Proceedings of the Royal Society of London, 71, p p. 421–426.

41. Owen, T., Mahaffy, P., Niemann, H. B., Atreya, S., Donahue, T., Bar-Nun, A. and De Pater, I. (1999). A low-temperature origin for the planetesimals that formed Jupiter. *Nature*, 402(6759) ,269–270.

42. Elena, A., Bolotnikov, A., Doke, E. and Tadayoshi (2006). Noble Gas Detectors. Weinheim, Wiley-VCH.

43. Caldwell, W. A., Nguyen, J., Pfrommer, B., . Louie, S. and Jeanloz, R. (1997). Structure, bonding and geochemistry of xenon at high pressures. *Science*, 277, 930–933

44. Anderson, J.S.M. and Ayers P.W. (2011). Quantum theory of atoms in molecules: results for the SR-ZORA Hamiltonian. *J Phys Chem A*., 115(45), 13001–13006

45. Filatov, M. and Cremer, D. (2003). On the physical meaning of the ZORA Hamiltonian. *Mol Phys*, 101(14), 2295–2302

46. Matito, E., Salvador, P. and Styszynski, J. (2013). Benchmark calculations of metal carbonyl cations: relativistic vs. electron correlation effects. *Phys Chem Chem Phys*, 15(46), 20080–20090.

47. Bučinský, L., Kucková, L., Malček, M., Kožíšek, J., Biskupič, S., Jayatilaka, D., ... & Arion, V. B. (2014). Picture change error in quasirelativistic electron/spin density, Laplacian and bond critical points. *Chemical Physics*, 438, 37-47.

48. Matta, C. F. and Boyd, R. J. (2007). An introduction to the quantum theory of atoms in molecules: from solid state to DNA and drug design. In: Matta CF, Boyd RJ (eds) The quantum theory of atoms in molecules. Wiley-VCH Verlag GmbH & Co. KGaA, Weinheim.

49. Fischer, C. F., Brage, T. and Jonsson, P. (2000). Computational Atomic Structure: An MCHF Approach. Institute of Physics Publishing Bristol and Philadlphia.

50. Grossetête, C. (1998). Restricted relativity and atomic structure of matter. Ellipses.

51. Gomis, L. (2008). Contribution to the study of the generalized oscillator forces in the length formulation and in the speed formulation. Application to the transitions of helium and neon. Doctoral thesis from, Cheikh Anta Diop University of Dakar.

52. Padma, R. and Deshmukh, P. C. (1992). Calculations of generalized oscillator strength for electron-impact excitations of krypton and xenon using a relativistic local-density potential. *Phys rev*, 46(5), 2513-2518.

53. Kohn, W. and Sham, L. J. (1965). Self-Consistent Equations Including Exchange and Correlation Effects. *Physi. Rev*, 140 (4), 1133–A1138.

54. Dirac, P. A. M. (1930). Note on Exchange Phenomena in the Thomas Atom. Proc. Camb. Phil. Soc. 26- 376.

55. Dahl, J. P. and Avery, J. (1984.). Local Density Approximations in Quantum Chemistry and Solid State. Physics, Plenum, New York.

56. Bunge, C. F. and Barrientos, J. A. (1993). Roothann-Hartree ground-state atomic wave functions Slater-Type orbital expansions and expectation values for Z=2-54 Atomic Data and Nuclear data Tables 53, Mexico: Instituto de Fisica, Universidad Nacional Autonoma de Mexico.